A molecular dynamics-informed probabilistic cross-slip model in discrete dislocation dynamics

Alon Malka-Markovitz, Benoit Devincre, Dan Mordehai

Scripta Materialia
Manuscript Draft

Manuscript Number: SMM-20-994

Title: A Molecular Dynamics-informed Probabilistic Cross-Slip Model in Discrete Dislocation Dynamics

Article Type: Regular article

Section/Category: Opt in to First Look

Keywords: Cross-slip
Discrete Dislocation Dynamics
Line tension model
Escaig stresses
Schmid stresses

Abstract: We present here a quantitative study of dislocation cross-slip, an essential thermally activated process in deformation of metals, in discrete dislocation dynamics (DDD) simulations. We implemented a stress-dependent line-tension model in DDD simulations, with minimal information from molecular dynamics (MD) simulations. This model allows reproducing in DDD simulations the probabilistic cross-slip rate calculated in MD simulations for Cu in a large range of stresses and temperatures. This model opens new horizons in modelling cross-slip related mechanisms such as deformation softening, dislocation-precipitate interaction and dislocation patterning in realistic strain rates.

A Molecular Dynamics-informed Probabilistic Cross-Slip Model in Discrete Dislocation Dynamics

Alon Malka-Markovitz[1]*, Benoit Devincre[2], Dan Mordehai[1]

[1]*Department of Mechanical Engineering, Technion—Israel Institute of Technology, 32000 Haifa, Israel*
[2]*LEM, UMR 104, CNRS-ONERA, 29 Av. de la Division Leclerc, Chatillon, France*

*Corresponding Author: alonma@campus.technion.ac.il

Abstract

We present here a quantitative study of dislocation cross-slip, an essential thermally activated process in deformation of metals, in discrete dislocation dynamics (DDD) simulations. We implemented a stress-dependent line-tension model in DDD simulations, with minimal information from molecular dynamics (MD) simulations. This model allows reproducing in DDD simulations the probabilistic cross-slip rate calculated in MD simulations for Cu in a large range of stresses and temperatures. This model opens new horizons in modelling cross-slip related mechanisms such as deformation softening, dislocation-precipitate interaction and dislocation patterning in realistic strain rates.

Keywords: Cross-slip, Discrete Dislocation Dynamics, Line tension model, Escaig stresses, Schmid stresses.

Mechanical properties of metals are mostly controlled by the evolution of their microstructure, mainly of the dislocation microstructure, a line defects network in the lattice structure. One of the main dislocation mechanisms is cross-slip, which is a thermally activated mechanisms by which screw dislocations can change their glide plane. For this reason, cross-slip is an essential mechanism in many mechanical processes, such as the decrease of the slope in stress-strain response correlated to a massive activity of dislocation cross-slip, known as Stage III Dynamic recovery of plasticity [1,2]. In addition cross-slip promotes annihilation of screw dislocations and internal stress relaxation, which contributes to the evolution of the dislocation density and has a vital role in patterning or cell formation [3–5] and even creep at intermediate and high temperatures [6,7]. Cross-slip modeling in face-centered cubic (FCC) metals is of particular interest since dislocations are dissociated and, in most cases, dislocations constrict during cross-slip, a process that requires overcoming a free-energy barrier.

Atomistic simulations are commonly employed to quantify the free-energy activation parameters for cross-slip. The a-thermal energy barrier for cross-slip is mainly calculated using the nudged elastic band (NEB) technique, which is a minimum energy path method to find the energy barrier between two microstates. Rasmussen et al. [8] used NEB simulations to calculate the activation energy for spontaneous annihilation of screw dislocations in a dipole structure, showing a good agreement with the Friedel-Escaig mechanism. Rao et al. [9] used the same technique to obtain the activation energy for Cu and Ni. Recently, Kang et al. [10] used the modified string method, another minimum energy path technique, to calculate the free energy barrier of a single screw dislocation in Ni under different stress conditions. In these simulations, the dependence of the free-energy barrier on several stress components was calculated.

In addition to the free-energy barrier, dynamic atomistic simulations are required to quantify the cross-slip rates. When high-enough stress is applied, the free-energy barrier becomes small enough to reproduce cross-slip in molecular dynamics (MD) simulations, which allows investigating cross-slip thermodynamics. Rao et al. and Vegge et al. used Molecular Dynamics (MD) simulations [11–14] to calculate the annihilation rate of an unstressed screw dislocation dipole. In these cases, small dislocation dipoles were considered, so that the interaction stress is high enough to trigger cross-slip. Cross-slip with larger dipoles in Cu were performed by Mordehai et

al. with applied external stresses to decrease the activation barrier [15]. Recently, Oren et al. [16] performed similar dipole annihilation simulations with longer dislocations of 200 b (~50 nm) length. In these simulations, that include several millions of atoms in each, a few hundred of simulations were performed in order to find from the probabilistic behavior of the results the dependence of the free-energy barrier for cross-slip on one stress component.

While atomistic simulations have proven themselves in capturing quantitatively the details for cross-slip, they are computationally expensive and even the largest atomistic simulations to date [17], are limited to a small fraction of 1μm^3, very high strain rates and focus on body-center cubic metals, in which the energy barrier for cross-slip is negligible. Therefore, it is desirable to employ the discrete dislocation dynamics (DDD) simulations which can be educated to reproduce at the mesoscopic scale some important properties simulated at the atomic scale and do the link between the atomic- and the continuum-level.

Cross-slip has been described in DDD simulation as a probabilistic mechanism [18], where probability of a screw dislocation segment of length L to cross-slip within a time step δt is

$$P = \alpha \frac{L}{L_0} e^{-\frac{H(\sigma)}{kT}} \delta t. \qquad (1)$$

$\boldsymbol{\sigma}$ is the stress tensor, α is a scaling rate factor (has units of frequency), L_0 is a reference length and kT has its usual meaning. Different DDD codes consider different forms for the free-energy barrier $H(\boldsymbol{\sigma})$. Most codes consider only the Schmid stresses (glide stresses) on the slip plane $\sigma_{sh.p}$ for an immobile dislocation, assuming that the activation energy is obtained from mainly from constricting the partial dislocations and it decreases linearly with this stress component: $H(\boldsymbol{\sigma}) = V_{sh}(\sigma_{sh.p} - \tau_{III})$ where τ_{III} is the resolved shear stress at the onset of Stage III of plasticity and V_{sh} is the corresponding activation volume. For a mobile dislocation, Brown equation is used, considering only Schmid stresses on the cross-slip plane $\sigma_{sh.cs}$ with a similar formulation [18]. The parameters of this model, including the value of α, were fitted to match experimental results of stage III of plasticity, rather than relying on information from the atomic scale. However, Hussein et al. [5] pointed out recently that Escaig stresses (non-glide stresses that controls the dissociation width) play a major

role. They proposed a linear dependence of the free-energy barrier on both Escaig stresses in the primary ($\sigma_{esc.p}$) and cross-slip ($\sigma_{esc.cs}$) planes: $H(\boldsymbol{\sigma}) = E_a - V_{esc}(\sigma_{esc.p} - \sigma_{esc.cs})$. E_a is the stress-free activation energy and V_{esc} is the activation volume that corresponds to both Escaig stresses. Both E_a and V_{esc} were argued to be extracted from MD simulations. Despite, this expression is inconsistent with NEB simulations, that shows different activation volumes for Escaig stresses in the different planes [10]. Also, such a linear expression fails to capture the divergence of the activation volume when $\sigma_{esc.p} < \sigma_{esc.cs}$. Finally, the model disregards the contribution of Schmid stress. All in all, neither model was shown to reproduce quantitively cross-slip rates in MD simulations in DDD simulations.

Recently, we proposed an expression for the stress dependent activation free energy barrier [19,20]. In this model, which is a line-tension model, we employed a harmonic approximation (HA) for the interaction energy between the partial dislocations and obtained a closed from expression for the activation energy for cross-slip of an unjogged dislocation via the Friedel-Escaig mechanism. The expression for the activation energy overcomes the drawbacks of previous models; it includes contributions of all stress components together, it generates a non-linear dependency as in the atomistic simulations, it diverges for $\sigma_{esc.p} < \sigma_{esc.cs}$ for $\sigma_{sh,cs} = 0$ etc. In what follows, we show here that when implemented in DDD simulations, with calibration of two parameters using MD simulation results, the model yields comparable results with MD simulations in a large range of temperatures and stresses. Such an implementation will allow simulating atomistic-based cross-slip behavior in more realistic strain rates, which are beyond the range commonly employed in MD simulations.

The free-energy barrier implemented in the DDD simulation relies on the line tension model [20]. Given that the stress field $\boldsymbol{\sigma}$ in the vicinity of a screw dislocation segment is known, three resolved stress components can be calculated: both Escaig stresses $\sigma_{esc,p}, \sigma_{esc,cs}$ and Schmid stress in the slip plane $\sigma_{sh,cs}$ (see Supplementary Information for details). Some DDD simulations include partial dislocations (e.g. [21]), which naturally captures these stress components. Still, in the vast majority of DDD simulations, dislocations are considered to be non-dissociated. While we detail in the Supplementary Information how the stress components are calculated for non-dissociated dislocations, we recall that dislocations are dissociated in FCC metals and the cross-slip model should account for the dissociated structure, even if not specifically

described in the DDD simulation. The equilibrium dissociation width on both primary and cross-slip planes are affected by Escaig stresses $\mathrm{d}_\sigma = \mathrm{d}_0\beta(\sigma_{esc})$ where d_0 is the stress-free dissociation width and $\beta(\sigma_{esc}) = \left(1 + \frac{\sqrt{3}b}{6\gamma}\sigma_{esc}\right)^{-1}$ (correspond both the primary and cross-slip planes, with the corresponding stress component). b is the Burgers vector of the whole dislocation and γ is the intrinsic stacking fault energy. In the Friedel-Escaig mechanism, the dislocation constricts at one point and then redissociates in the cross-slip plane. At the peak of the energy barrier, the length of dislocation that redissociated into the cross-slip plane l_c satisfies the equation

$$\frac{1.55}{(cosh(l_c))^2} - \frac{3\delta}{\beta_{cs}}(l_c)^2 = 2\mathrm{E}^*,$$

where $\mathrm{E}^* = \ln\left(\frac{\mathrm{d}_{\sigma,\mathrm{cs}}}{\mathrm{d}_{\sigma,\mathrm{p}}}\right)$ is the off-set in the interaction energies between the primary and cross-slip planes, $\delta = \frac{1}{6}\left(\frac{b\sigma_{sh,cs}}{\gamma}\right)^2$. Given than the value of l_c is found, the activation energy is

$$H(\boldsymbol{\sigma}) = E_0\left\{\frac{\beta_p}{2} + \left(\frac{\beta_{cs}}{2}\right)\left[tanh(l_c) - \frac{2\alpha_{\mathrm{Ls}}}{1.55}l_c\mathrm{E}^* - \frac{(\alpha_{\mathrm{Ls}})^3}{1.55}\frac{\delta}{\beta_{cs}}{l_c}^3\right]\right\} \qquad (2)$$

where, E_0 is the unstressed activation energy for cross-slip, considered here as a fitting parameter and $\alpha_{\mathrm{Ls}} = 0.6$.

The energy barrier was applied in the DDD code MicroMegas. A probabilistic Monte-Carlo cross-slip mechanism, of the form of Eq.(2), was implemented with the energy form given in Eq. 0. Additionally, the value of L_0 is taken as b since cross-slip can commence at any L/b sites along the dislocation segment. As a result, α becomes the attempt rate for cross-slip at one of the sites along the dislocation line.

The values of E_0 and α for Cu were fitted based on Molecular Dynamic (MD) simulation results. Oren et al. [16] published a detailed series of MD simulations from which the annihilation rate of unjogged screw dislocations in a dipole structure was calculated. The distance between the two primary slip planes of the dislocations in the dipole, denoted here as dipole size, is 20b. A series of MD simulations at different temperatures T and external shear stresses σ_{ext} were performed and the reaction rate for the annihilation of a screw dipole with cross-slip as a function of temperature and stress $k(T, \sigma_{ext})$ was calculated from the reaction time distribution. While most of the

rates were calculated for an effective dislocation length of $200b$, the dependence of the rate on the dislocation length was also calculated.

In the present study, similar configurations were investigated with DDD simulations. A simulation volume of size of 361 x 722 x 361nm and periodic boundary conditions in cubic directions was considered. The simulation box is fully periodic. As illustrated in Fig. 1 and similarly to the configuration used in the MD simulations, two screw dislocations in a dipole configuration are initially set in the simulation volume, with a dipole size of 20b and a dislocation length of 200b. Since the dipole in the MD was aligned parallel to the transverse slip plane, e.g. a stable configuration for nearby dissociated dislocations, the same initial configuration was used in the DDD simulations. It should be noted here that this configuration is in isotropic elasticity unstable for constricted dislocations, for this reason the dislocations were forced in DDD simulations not to glide in their primary slip plane.

As in the MD simulations, an external shear stress σ_{ext} that yields an Escaig stress in the primary and cross-slip planes is applied. However, the dissociated partial dislocations simulated with MD simulations are sources of internal stresses that are not reflected in the DDD simulations when considering non-dissociated dislocations. As discussed in [22], such contributions coming from the dissociation are significant for close dislocations and lead to variations of the Escaig and Schmid stresses of the order of a few hundreds of MPa. Based on calculations using isotropic elasticity theory and accounting for the dissociation width observed in MD, in dipole size considered here the Escaig stress lost when considering non-dissociated dislocations is around $\sigma_{esc,p}$~430 MPa in the primary slip plane and $\sigma_{esc,cs}$~334 MPa in the cross-slip plane. The contribution of the internal Schmid stress was found to be small in [22] and it is neglected here. Therefore, in the DDD calculations, a stress shift of 430 MPa is taken into account for the applied shear stress in order to compensate the absent dissociation effects, i.e., when a stress of 1.53 GPa is applied in the DDD, it corresponds approximately to an external shear stress of 1.1 GPa in the MD calculations.

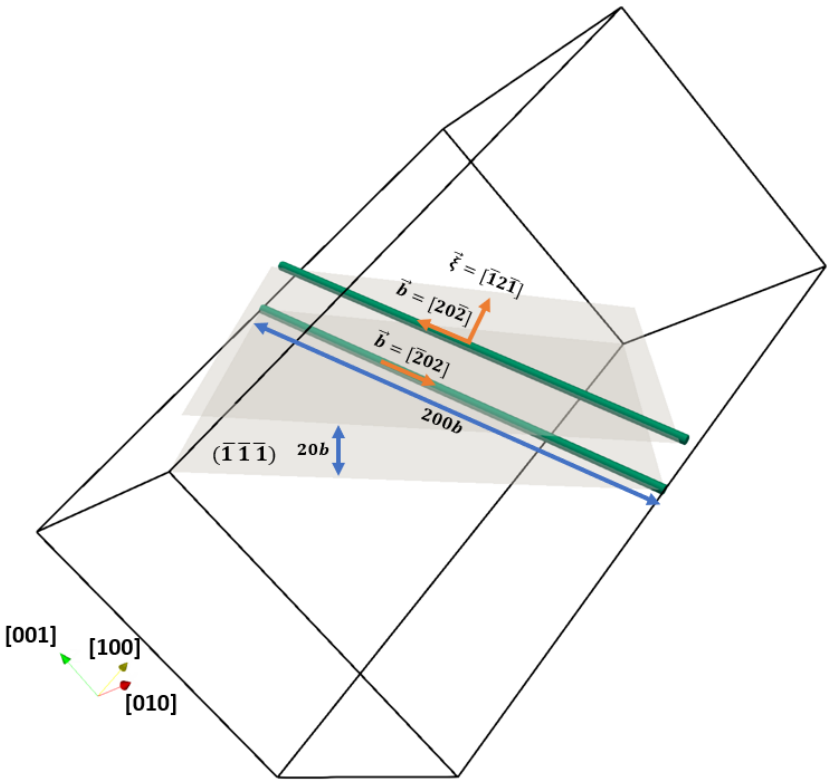

Fig. 1: MicroMegas Simulation Setup of a dislocation dipole with a dipole size of 20b (distance between the primary slip planes) and dislocations of length 200b.

For each set of parameters, the simulations were repeated $N_0 = 40$ times, in order to explore the stochastic cross-slip mechanism. To demonstrate the probabilistic behavior of the simulations, we plot in Fig. 2 the fraction of simulations N/N_0 without cross-slip until time t, for an external stress of 1.1 GPa and a temperature of 525K for different dislocation lengths (simulation box was adapted to the specific dislocation length to enable full periodicity of each simulation dipole set). Uncalibrated values of $\alpha = 8.8 \cdot 10^{13}\ 1/s$ and $E_0 = 1.55\ eV$ were considered and the simulations are repeated for different dislocation lengths. This probabilistic behavior is very similar to one found in the MD simulations. Firstly, the fraction of DDD simulations in which cross-slip did not occur is decreasing exponentially with time. Oren et al. proposed that the fraction N/N_0 is related to the cross-slip rate k via first order reaction kinetics

$$N/N_0 = e^{-kt} \qquad (3)$$

Using this relation, the cross-slip rate was derived from each plot. In the inset of Fig. 2, we demonstrate the increase of the cross-slip rate as a function of the length of the dislocation. The values of k increase rather linearly with the length, as expected.

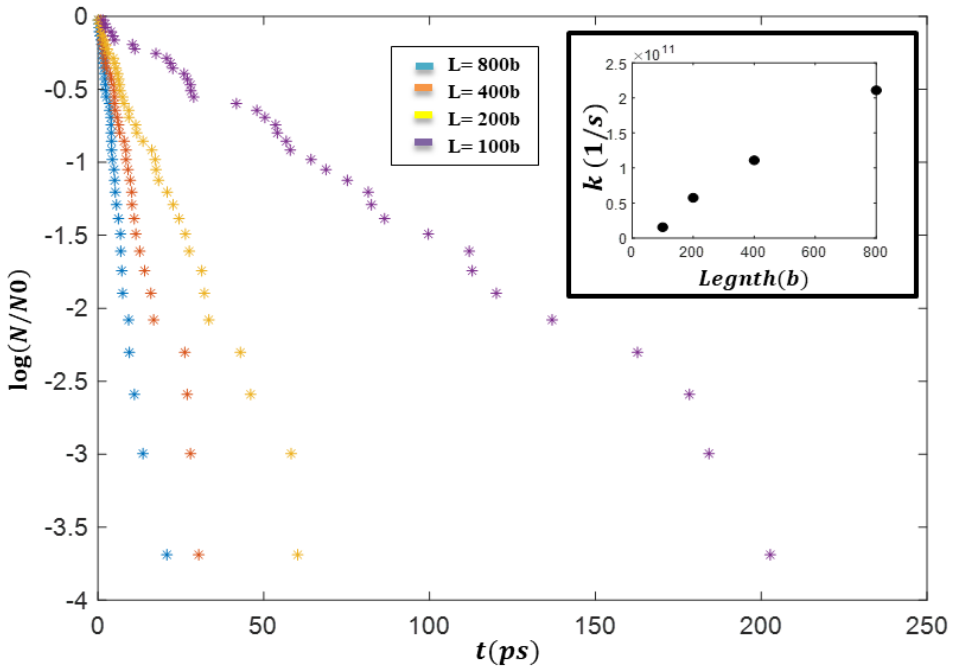

Fig. 2: The evolution of the fraction of simulations without a cross-slip event at $\sigma_{ext} = 1.1GPa$ and $T = 525K$. The increase of the cross-slip rate as a function of the length of the dislocation is plotted in the inset.

In what follows, we fixed the dislocations length to 200b, as in the MD simulations. In order to calibrate the DDD simulations, we adjusted both E_0 and v_0 to match with the cross-slip rates found in MD simulations. The cross-slip is satisfying an Arrhenius law of the form

$$k(T, \sigma_{ext}) = v_0 e^{-E_{act}(\sigma_{ext})/K_B T} \qquad (4)$$

where v_0 is an attempt rate, that depends linearly on the dislocation length as shown in Fig. 2. For given values of E_0 and α, the cross-slip rate as function of external stress and temperature is calculated. Based on Eq. (4), the slope of the relation $\ln(k) - (k_B T)^{-1}$ corresponds to the activation energy and not to the attempt rate. For this reason, E_0 was calibrated using the slope of the plot of ln(k) as a function of $(k_B T)^{-1}$ and α was later adjusted to fit one of the values. The value of E_0 was chosen so that the slope of the relation $\ln(k) - (k_B T)^{-1}$ for an external stress of 1.1 GPa is comparable with the MD simulation results ($E_{act} = 0.37\ eV$) and α was fitted independently to the value of k for a stress of 1.1 GPa and a temperature of 425K ($k = 2.9 \cdot 10^9\ 1/s$). The

calibration process yielded values of $\alpha = 2 \cdot 10^{12}\ 1/s$ and $E_0 = 1.55\ eV$. We note that the value of α is an order of magnitude smaller than Debye frequency ($\sim 10^{13}\ 1/s$), which agrees with processes that involves group of atoms (like dislocation nucleation [23]).

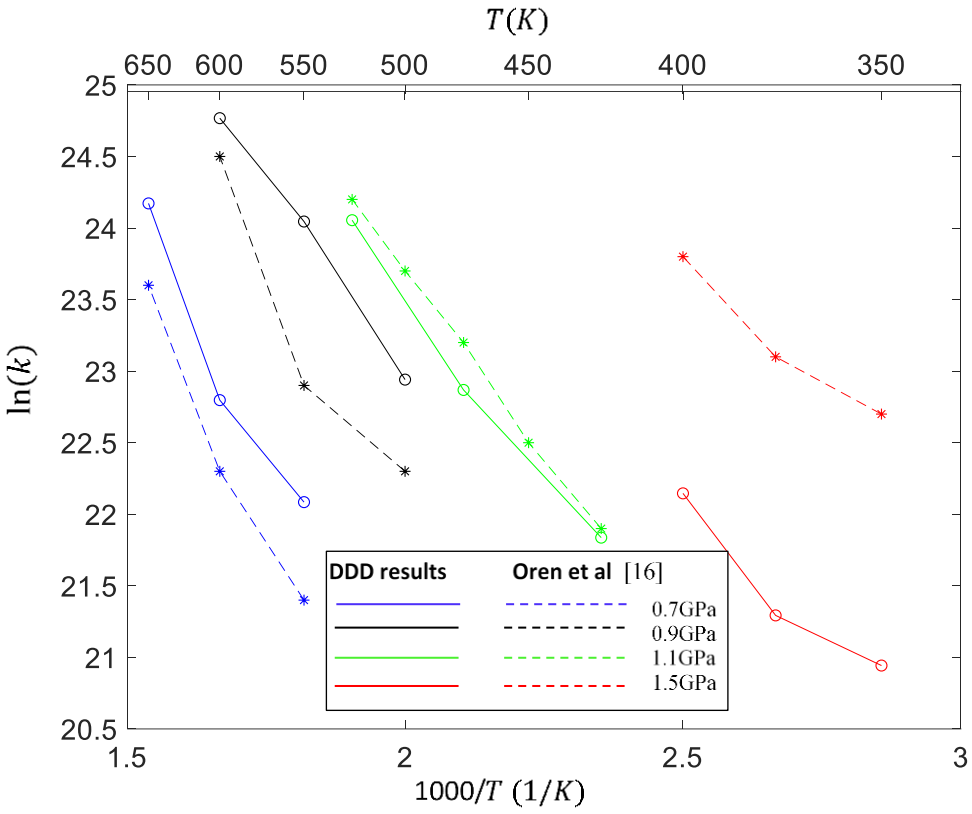

Fig. 3: Variation of ln (k) as a function of the external stress and temperature with $E_0 = 1.55eV$ and $\alpha = 2 \cdot 10^{12}\ s^{-1}$ 1/s. k is in units of $1/s$. The slope of MD simulation results of Oren et al [16] at 1.1 GPa was used calibrate E_0, and the value of k in 425K was used to calibrate α.

Using the fitted value, we performed DDD simulations at various stress levels and temperatures. Then we calculated the cross-slip rate (for each stress and temperature, the procedure described in Fig. 2 was repeated, with 40 simulations). As can be seen from Fig. 3, the value of the cross-slip rate is increasing with temperature and higher stresses also increase the rate. More profoundly, this DDD simulations are shown to be in an excellent agreement with the MD simulation results at a large range of stresses and temperatures. At the highest stress, the cross-slip rate in the DDD was found to be

smaller by an order of magnitude. To explain this, the activation energies were calculated from the line tension model (Eq. (2)) and were compared with the values obtained from the MD simulations. The comparison is shown in Fig. 4. One can see that the values are comparable but at the largest external stress the DDD captures a higher energy barrier for cross-slip, and at lower stress the DDD underestimates the energy barrier (although, within the error bar of the MD simulation results).

Several modifications can improve the accuracy of the DDD simulations. For instance, the material parameters considered in the simulations are temperature-independent, while the elastic constants are temperature dependent. In particular, C_{44} in Cu differs by about 10% in the range of temperatures examined here [24]. This affects both the elastic interaction between the partial dislocations and the internal Escaig stresses. While the contribution of the temperature to each material property may be complex, its total contribution on the equilibrium dissociation width was also examined in the MD simulations or Oren et al. [16], and it was found that without an external Escaig stress the dissociation width increases with temperature by about 10% in a range of 500 K. Considering a larger dissociation width will require more work to cross-slip, i.e., such a correction will bring the activation energy in DDD closer to the MD simulation results at the lower stresses. Additionally, at an external Escaig stress of 1.5 GPa, the dissociation width decreases with temperature by about 10% in the same temperature range, which may lower the activation energy at higher stresses. Thus, considering temperature-dependent material properties may bring the DDD results in Fig. 4 closer to the MD simulation results. Additionally, the cross-slip model implemented here considers a homogenous line tension, while an orientation-dependent line-tension expression may even improve the comparison with the energy barrier calculated in atomistic simulations [25] . Nevertheless, given the simplicity of the line tension model presented here, one can obtain comparable results between MD and DDD simulations, which allow pushing the limits of simulating cross-slip in realistic strain rates.

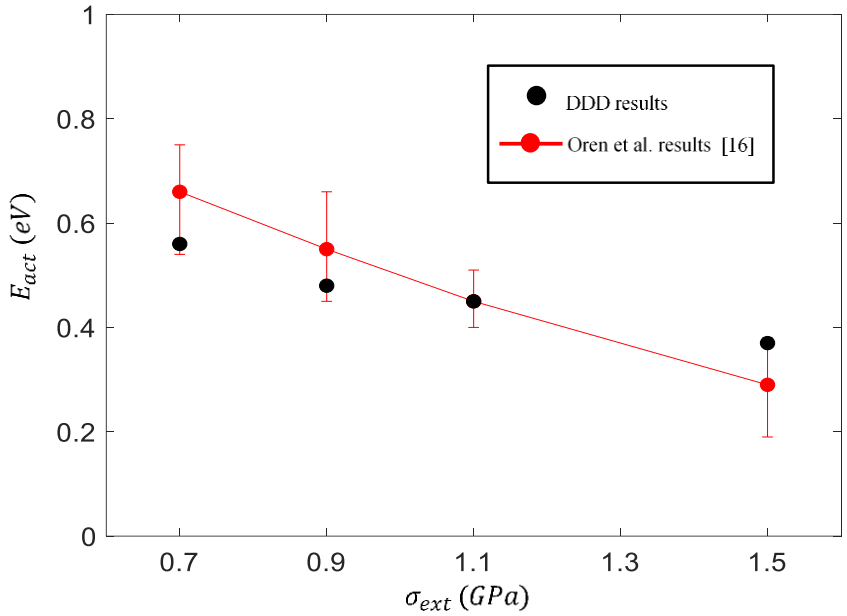

Fig. 4: Oren et al. [16] results in comparison with the DDD results for the activation energy at different external shear stresses. The value at 1.1 GPa is the calibrated one.

In summary, we implemented a stress-dependent line tension model in DDD simulations and showed that with minimal information from MD simulations, it can capture accurately the probabilistic behavior of cross-slip in a large range of stresses and temperatures. This model, which is easy to implement, allows overcoming the cumbersome atomistic simulations required to study cross-slip and promote the ability to perform simulations in larger systems and smaller strain rates than the one accessible by atomistic simulations. While the model is based on the line tension model for unjogged dislocations, extensions for jogged dislocations or cross-slip near surface is possible. Those will result in different values for E_0 and α, as it is known that jogs and surface reduce the energy barrier for cross-slip. The incorporation of all stress components in the cross-slip model will allow examining more realistic cases in which cross-slip is essential to study mechanical properties of metals and microstructure evolution, such as dislocation-precipitate interaction [26], dislocation patterning [27] high strain-rate deformation [28] etc.

References

P. J. Jackson, Prog. Mater. Sci. **29**, 139 (1985). [1]

E. I. Galindo-Nava and P. E. J. Rivera-Díaz-del-Castillo, Int. J. Plast. **47**, 202 (2013). [2]

L. P. Kubin, G. Canova, M. Condat, B. Devincre, V. Pontikis, and Y. Bréchet, Solid State Phenom. **23**–**24**, 455 (1992). [3]

C. Déprés, C. F. Robertson, and M. C. Fivel, Philos. Mag. **86**, 79 (2006). [4]

A. M. Hussein, S. I. Rao, M. D. Uchic, D. M. Dimiduk, and J. A. El-Awady, Acta Mater. **85**, 180 (2015). [5]

J. P. Poirier, Rev. Phys. Appliquée **11**, 731 (1976). [6]

D. Caillard and J.-L. Martin, *Thermally Activated Mechanisms in Crystal Plasticity* (Pergamon, Amsterdam, 2003). [7]

T. Rasmussen, T. Leffers, O. B. Pedersen, K. W. Jacobsen, B. Pedersen, and K. W. Jacobsens, Philos. Mag. A **80**, 1273 (2000). [8]

S. I. Rao, D. M. Dimiduk, T. A. Parthasarathy, J. El-Awady, C. Woodward, and M. D. Uchic, Acta Mater. **59**, 7135 (2011). [9]

K. Kang, J. Yin, and W. Cai, J. Mech. Phys. Solids **62**, 181 (2014). [10]

S. I. Rao, D. M. Dimiduk, T. a. Parthasarathy, M. D. Uchic, and C. Woodward, Scr. Mater. **66**, 410 (2012). [11]

S. I. Rao, D. M. Dimiduk, T. A. Parthasarathy, M. D. Uchic, and C. Woodward, Acta Mater. **61**, 2500 (2013). [12]

T. Vegge, Mater. Sci. Eng. A **309**–**310**, 113 (2001). [13]

T. Vegge, T. Rasmussen, T. Leffers, O. B. Pedersen, and K. W. Jacobsen, Philos. Mag. Lett. **81**, 137 (2001). [14]

D. Mordehai, I. Kelson, and G. Makov, Mater. Sci. Eng. A **400**–**401**, 37 (2005). [15]

E. Oren, E. Yahel, and G. Makov, Comput. Mater. Sci. **138**, 246 (2017). [16]

L. A. Zepeda-Ruiz, A. Stukowski, T. Oppelstrup, and V. V. Bulatov, Nature **550**, 492 (2017). [17]

B. Devincre, R. Madec, G. Monnet, S. Queyreau, R. Gatti, and L. Kubin, in *Mech. Nano-Objects*, edited by O. Thomas, A. Ponchet, and S. Forest (Presses de l'Ecole des Mines de Paris, Paris, 2011), pp. 81–100. [18]

A. Malka-Markovitz and D. Mordehai, Philos. Mag. **98**, 347 (2018). [19]

A. Malka-Markovitz and D. Mordehai, Philos. Mag. 1 (2019). [20]

E. Martínez, J. Marian, A. Arsenlis, M. Victoria, and J. M. Perlado, J. Mech. Phys. Solids **56**, 869 (2008). [21]

A. Malka-Markovitz and D. Mordehai, Philos. Mag. **99**, 1460 (2019). [22]

D. Chachamovitz and D. Mordehai, Sci. Rep. **8**, 3915 (2018). [23]

Y. A. Chang and L. Himmel, J. Appl. Phys. **37**, 3567 (1966). [24]

H. Liu, X. Zhou, D. Hu, J. Song, R. Wang, and J. Mao, Scr. Mater. **166**, 24 (2019). [25]

C. V. Singh, A. J. Mateos, and D. H. Warner, Scr. Mater. **64**, 398 (2011). [26]

P. Landau, D. Mordehai, A. Venkert, and G. Makov, Scr. Mater. **66**, 135 (2012). [27]

Z. Q. Wang, I. J. Beyerlein, and R. LeSar, Model. Simul. Mater. Sci. Eng. **15**, 675 (2007). [28]

Supplementary Material

Click here to download Supplementary Material: A_Molecular_Dynamics__Supp.pdf

*Graphical Abstract